Pergamon

0956-7151(94)00484-6

Acta metall. mater. Vol. 43, No. 8, pp. 3177–3184, 1995
Elsevier Science Ltd
Copyright © 1995. Acta Metallurgica Inc.
Printed in Great Britain. All rights reserved
0956-7151 95 $9.50 + 0.00

A CRYSTAL PLASTICITY VIEW OF POWDER COMPACTION

N. A. FLECK

Department of Engineering, University of Cambridge, Trumpington Street, Cambridge CB2 1PZ, England

(Received 9 September 1994)

Abstract—The cold compaction of an aggregate of powder is treated from the viewpoint of crystal plasticity theory. The contacts between particles are treated as compaction planes which yield under both normal and shear straining. The hardening of each plane represents both geometric and material hardening at the contacts between particles; the macroscopic tangent stiffness can be written in terms of the hardening rate for active compaction planes. During the early stages of compaction the contacts yield in an independent manner, which can be interpreted within the crystal context as independent hardening. The macroscopic yield surfaces for isostatic and closed die compaction are estimated for a uniform distribution of an orthogonal pair of compaction planes. A vertex forms at the loading point and significant anisotropy develops for closed die compaction.

1. INTRODUCTION

The powder metallurgy industry is based upon the process of cold compaction of powders (usually, but not exclusively metallic) followed by sintering. This production route allows for the net shape forming of exotic alloys which are difficult to cast or shape by other methods. Cold compaction occurs within a closed die or in a cold isostatic press, and densification is by low temperature plasticity. At low relative densities (relative density, $D < 0.9$) plastic deformation occurs local to the contacts between particles: this is "Stage I" compaction. As full density is approached "Stage II" compaction takes over and plastic flow spreads throughout each particle; then, the powder aggregate is best viewed as a non-dilute concentration of cusp-shaped voids within a metallic matrix.

In this paper we consider Stage I compaction within the framework of crystal plasticity theory. The central idea is to mimic the response at a contact between particles by a "compaction plane", that is by a plane which can suffer both normal and shear straining (see Fig. 1). We consider the compaction plane to be smeared out through the volume of the neighbouring particles on each side of the contact, but sharing the same normal n as that of the contact plane, as shown in Fig. 1(a). In this manner the compaction plane is analogous to a slip plane in crystal plasticity theory. Each contact is represented by a compaction plane, and the overall response of the aggregate is the sum of the responses of each compaction plane. The approach builds upon Calladine's micromechanical model of the yielding of clays [1]. He assumed that compaction planes exist physically as rough surfaces of contact within the aggregate, the depth of the roughness being related to the size of the voids in the aggregate. Here, we consider the compaction planes to represent discrete contacts between the particles.

The outline of the paper is as follows. First, a single crystal plasticity framework is summarised for a finite number of compaction planes. The Bishop and Hill [2] method is then used to determine the macroscopic limit yield surface for a "polycrystal" wherein each crystal comprises a pair of orthogonal compaction planes. The normal to the compaction planes is averaged over all orientations n within a plane, and the polycrystal is subjected to macroscopic in-plane biaxial loading. Using the crystal plasticity framework the effect of strain path upon yield surface evolution is explored by comparing the yield surfaces for isostatic compaction and closed die compaction. The marked development of anisotropy is evident for closed die compaction.

2. CRYSTAL PLASTICITY FRAMEWORK

We replace each contact between particles by a compaction plane within the particle. In this way the finite number of contacts around a representative particle are represented by a finite number of compaction planes within the particle: the particle is analogous to a single crystal with a set of slip planes.

Consider a representative contact with normal $n^{(1)}$ as shown in Fig. 1(a). The neighbouring particles on each side of this contact can suffer a relative displacement in a direction parallel to $n^{(1)}$, and a shear displacement orthogonal to $n^{(1)}$. The resulting contact force between the particles depends upon the deformation mechanism at the contact; here we shall assume a non-linear response due to plastic dissipation. The non-linear contact law between the

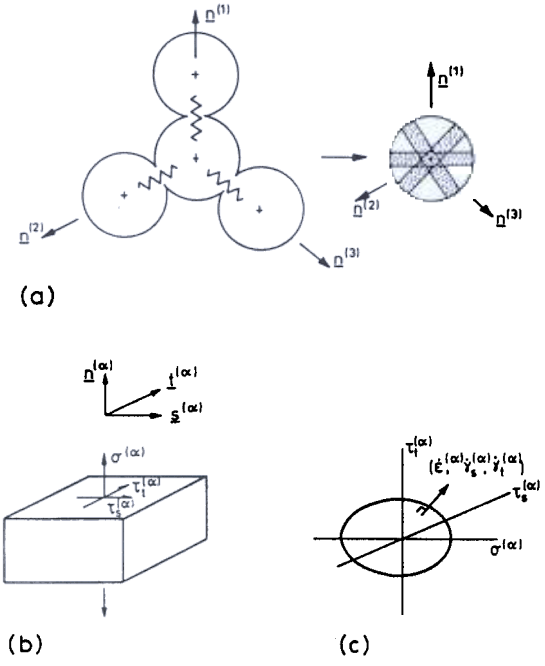

Fig. 1. (a) Representation for the isolated contacts between particles by "smeared-out" compaction planes. (b) Loading on a compaction plane (α). (c) Yield surface and normal plastic flow rule for a compaction plane (α).

neighbouring particles can be treated as a non-linear spring at the contact, or as a "smeared-out" compaction plane over the volume of each particle.

A representative compaction plane α is defined in Fig. 1(b). The smeared-out plane is allowed to suffer a normal strain $\epsilon^{(\alpha)}$ in the direction $n^{(\alpha)}$ and two shear strains $\gamma_s^{(\alpha)}$ and $\tau_t^{(\alpha)}$ in the directions $s^{(\alpha)}$ and $t^{(\alpha)}$, respectively. These strains act over the volume of the particle and give rise to the same displacement at the contact as the non-linear spring representation. We shall assume that strains are small, and shall neglect the effects of finite rotation of the compaction planes. A finite strain generalisation can be developed in a relatively straightforward manner, but is omitted here.

The work conjugate stress measures are the normal stress $\sigma^{(\alpha)}$ and two shear stresses $\tau_s^{(\alpha)}$ and $\tau_t^{(\alpha)}$, such that the work rate per unit volume $w^{(\alpha)}$ is

$$w^{(\alpha)} = \sigma^{(\alpha)}\dot{\epsilon}^{(\alpha)} + \tau_s^{(\alpha)}\dot{\gamma}_s^{(\alpha)} + \tau_t^{(\alpha)}\dot{\gamma}_t^{(\alpha)} \tag{2.1}$$

where no sum is performed over the index α unless explicitly stated by a summation sign. Suppose the aggregate is comprised of N compaction planes. Then, in terms of the Cartesian reference frame x_i, the macroscopic plastic strain rate $\dot{E}_{ij}^p$ is related to the strain rate $(\dot{\epsilon}^{(\alpha)}, \dot{\gamma}_s^{(\alpha)}, \dot{\gamma}_t^{(\alpha)})$ on each active compaction plane α by

$$\dot{E}_{ij}^p = \sum_{\alpha=1}^{N} [P_{ij}^{(\alpha)}\dot{\epsilon}^{(\alpha)} + Q_{ij}^{(\alpha)}\dot{\gamma}_s^{(\alpha)} + R_{ij}^{(\alpha)}\dot{\gamma}_t^{(\alpha)}] \tag{2.2}$$

where the orientation factors $P_{ij}^{(\alpha)}$, $Q_{ij}^{(\alpha)}$ and $R_{ij}^{(\alpha)}$ are defined by

$$P_{ij}^{(\alpha)} \equiv n_i^{(\alpha)} n_j^{(\alpha)}, \qquad Q_{ij}^{(\alpha)} \equiv \tfrac{1}{2}(n_i^{(\alpha)} s_j^{(\alpha)} + s_i^{(\alpha)} n_j^{(\alpha)}),$$

$$R_{ij}^{(\alpha)} \equiv \tfrac{1}{2}(n_i^{(\alpha)} t_j^{(\alpha)} + t_i^{(\alpha)} n_j^{(\alpha)}).$$

The macroscopic stresses on each compaction plane $(\sigma^{(\alpha)}, \tau_s^{(\alpha)}, \tau_t^{(\alpha)})$ are related to the macroscopic stress Σ by substituting equation (2.2) into the work statement

$$\Sigma_{ij}\dot{E}_{ij}^p = \sum_{\alpha=1}^{N} [\sigma^{(\alpha)}\dot{\epsilon}^{(\alpha)} + \tau_s^{(\alpha)}\dot{\gamma}_s^{(\alpha)} + \tau_t^{(\alpha)}\dot{\gamma}_t^{(\alpha)}]$$

to get

$$\sigma^{(\alpha)} = P_{ij}^{(\alpha)}\Sigma_{ij}, \qquad \tau_s^{(\alpha)} = Q_{ij}^{(\alpha)}\Sigma_{ij}$$

and

$$\tau_t^{(\alpha)} = R_{ij}^{(\alpha)}\Sigma_{ij}.$$

We assume that a compaction plane α plastic flow when the yield function

$$f^{(\alpha)} \equiv \sigma_e^{(\alpha)}(\sigma^{(\alpha)}, \tau_s^{(\alpha)}, \tau_t^{(\alpha)}) - \sigma_Y^{(\alpha)} = 0 \tag{2.6}$$

is satisfied. Here, $\sigma_e^{(\alpha)}$ is an effective stress measure and $\sigma_Y^{(\alpha)}$ is a scalar measure of the current magnitude of the yield surface. The shape of the yield surface is dependent upon the local contact law between particles, including the shear strength and the cohesive strength. For example, a yield surface of elliptical shape is given by

$$\sigma_e^{(\alpha)} = \sqrt{(\sigma^{(\alpha)})^2 + (a^{(\alpha)}\tau_s^{(\alpha)})^2 + (b^{(\alpha)}\tau_t^{(\alpha)})^2} \tag{2.7}$$

where $a^{(\alpha)}$ and $b^{(\alpha)}$ are constants defining the ellipticity of the yield surface. Here, we shall continue to work in terms of the general form of equation (2.6) rather than the particular form of equation (2.7).

For simplicity, we assume that plastic flow occurs in a direction normal to the yield surface for each compaction plane, giving

$$\dot{\epsilon}^{(\alpha)} = \lambda^{(\alpha)}\frac{\partial\sigma_e^{(\alpha)}}{\partial\sigma^{(\alpha)}}, \qquad \dot{\gamma}_s^{(\alpha)} = \lambda^{(\alpha)}\frac{\partial\sigma_e^{(\alpha)}}{\partial\tau_s^{(\alpha)}}$$

and

$$\dot{\gamma}_t^{(\alpha)} = \lambda^{(\alpha)}\frac{\partial\sigma_e^{(\alpha)}}{\partial\tau_t^{(\alpha)}}$$

The magnitude of the plastic multiplier $\lambda^{(\alpha)}$ is determined from a work hardening statement, as follows. Introduce an effective strain rate $\dot{\epsilon}_e^{(\alpha)}$ by the work statement

$$w^{(\alpha)} \equiv \sigma_e^{(\alpha)}\dot{\epsilon}_e^{(\alpha)} = \sigma^{(\alpha)}\dot{\epsilon}^{(\alpha)} + \tau_s^{(\alpha)}\dot{\gamma}_s^{(\alpha)} + \tau_t^{(\alpha)}\dot{\gamma}_t^{(\alpha)}. \tag{2.9}$$

Then, upon substituting equation (2.8) into equation (2.9), $\lambda^{(\alpha)}$ is expressible in terms of $\dot{\epsilon}_e^{(\alpha)}$ as

$$\lambda^{(\alpha)} = C^{(\alpha)}\dot{\epsilon}_e^{(\alpha)} \tag{2.10}$$

where

$$C^{(\alpha)} \equiv \frac{\sigma_e^{(\alpha)}}{\sigma^{(\alpha)}\dfrac{\partial \sigma_e^{(\alpha)}}{\partial \sigma^{(\alpha)}} + \tau_s^{(\alpha)}\dfrac{\partial \sigma_e^{(\alpha)}}{\partial \tau_s^{(\alpha)}} + \tau_t^{(\alpha)}\dfrac{\partial \sigma_e^{(\alpha)}}{\partial \tau_t^{(\alpha)}}}. \tag{2.11}$$

[It is noted that $C^{(\alpha)} = 1$ when $\sigma_e^{(\alpha)}$ is homogeneous and of degree one in $(\sigma^{(\alpha)}, \tau_s^{(\alpha)}, \tau_t^{(\alpha)})$ such as given by equation (2.7).] The macroscopic plastic strain rate can now be expressed in terms of the effective strain rate on each compaction plane $\dot{\epsilon}_e^{(\alpha)}$ by rewriting equation (2.2) with the aid of equation (2.8) and (2.10) as

$$\dot{E}_{ij}^p = \sum_{\alpha=1}^{N} [C^{(\alpha)} T_{ij}^{(\alpha)} \dot{\epsilon}_e^{(\alpha)}] \tag{2.12}$$

where

$$T_{ij}^{(\alpha)} \equiv \frac{\partial \sigma_e^{(\alpha)}}{\partial \sigma^{(\alpha)}} P_{ij}^{(\alpha)} + \frac{\partial \sigma_e^{(\alpha)}}{\partial \tau_s^{(\alpha)}} Q_{ij}^{(\alpha)} + \frac{\partial \sigma_e^{(\alpha)}}{\partial \tau_t^{(\alpha)}} R_{ij}^{(\alpha)}. \tag{2.13}$$

The overall hardening law is specified by

$$\dot{\sigma}_e^{(\alpha)} = \sum_{\beta=1}^{N} [h_{\alpha\beta} \dot{\epsilon}_e^{(\beta)}]. \tag{2.14}$$

In general, the hardening matrix $h_{\alpha\beta}$ can be homogeneous and of degree zero in the effective strain rates $\dot{\epsilon}_e^{(\alpha)}$; here, only hardening laws for which the $h_{\alpha\beta}$ are independent of the effective strain rates are employed.

Let $\mathscr{L}$ be the macroscopic elastic stiffness tensor and $\mathscr{M} = \mathscr{L}^{-1}$ be the macroscopic elastic compliance tensor. Then, the total strain rate $\dot{E}_{ij}$ is related to $\mathring{\Sigma}_{ij}$ by

$$\mathring{\Sigma}_{ij} = \mathscr{L}_{ijkl}(\dot{E}_{kl} - \dot{E}_{kl}^p) \tag{2.15}$$

and by

$$\dot{E}_{ij} = \mathscr{M}_{ijkl}\mathring{\Sigma}_{kl} + \dot{E}_{ij}^p. \tag{2.16}$$

Next, assume that $\mathscr{M}$ and $h_{\alpha\beta}$ are positive definite. Then, following an argument of Hill [3]

(i) if $\mathring{\Sigma}_{ij}$ is prescribed then $\dot{E}_{ij}$ and the strain rates $(\dot{\epsilon}^{(\alpha)}, \dot{\gamma}_s^{(\alpha)}, \dot{\gamma}_t^{(\alpha)})$ are unique, and

(ii) if $\dot{E}_{ij}$ is prescribed then $\mathring{\Sigma}_{ij}$ and the strain rates $(\dot{\epsilon}^{(\alpha)}, \dot{\gamma}_s^{(\alpha)}, \dot{\gamma}_t^{(\alpha)})$ are unique.

In order to implement the above crystal plasticity law the macroscopic tangent modulus L is required, where L is defined by

$$\mathring{\Sigma}_{ij} = L_{ijkl}\dot{E}_{kl}. \tag{2.17}$$

An explicit expression for L is obtained by rearranging equation (2.15) into equation (2.17) by using equation (2.12)

$$\mathring{\Sigma}_{ij} = \mathscr{L}_{ijkl}\dot{E}_{kl} - \sum_{\alpha=1}^{N} [\mathscr{L}_{ijkl} T_{kl}^{(\alpha)} C^{(\alpha)} \dot{\epsilon}_e^{(\alpha)}]. \tag{2.18}$$

To proceed, we establish a connection between $\dot{\epsilon}_e^{(\alpha)}$ and $\dot{E}_{ij}$. The effective stress rates $\dot{\sigma}_e^{(\alpha)}$ are expressed in terms of $\mathring{\Sigma}_{ij}$ using equations (2.5), (2.6) and (2.13) to give

$$\dot{\sigma}_e^{(\alpha)} = T_{ij}^{(\alpha)}\mathring{\Sigma}_{ij}. \tag{2.19}$$

With the aid of equations (2.14) and (2.15) this leads to a connection between the strain rates $\dot{\epsilon}_e^{(\alpha)}$ and $\dot{E}_{ij}$ as

$$\dot{\sigma}_e^{(\alpha)} = \sum_{\beta=1}^{N} [h_{\alpha\beta}\dot{\epsilon}_e^{(\beta)}] = T_{ij}^{(\alpha)}\mathring{\Sigma}_{ij} = T_{ij}^{(\alpha)}\mathscr{L}_{ijkl}(\dot{E}_{kl} - \dot{E}_{kl}^p) \tag{2.20}$$

or, upon substituting equation (2.12) for $\dot{E}_{ij}^p$

$$T_{ij}^{(\alpha)}\mathscr{L}_{ijkl}\dot{E}_{kl} = \sum_{\beta=1}^{N} [N_{\alpha\beta}\dot{\epsilon}_e^{(\beta)}] \tag{2.21}$$

where

$$N_{\alpha\beta} \equiv h_{\alpha\beta} + T_{ij}^{(\alpha)}\mathscr{L}_{ijkl}T_{kl}^{(\beta)}C^{(\beta)}. \tag{2.22}$$

The sum in equation (2.21) is taken over all active compaction planes, for which $\dot{\epsilon}_e^{(\alpha)} > 0$. For a given strain rate $\dot{E}_{ij}$ we assume that the active compaction planes are known, so that the effective strain rates $\dot{\epsilon}_e^{(\alpha)}$ can be calculated from equation (2.21). This calculation requires the matrix $N_{\alpha\beta}$ to be inevitable which is presumed the case. Then

$$\dot{\epsilon}_e^{(\alpha)} = \sum_{\beta=1}^{N} [(N^{-1})_{\alpha\beta} T_{ij}^{(\beta)}\mathscr{L}_{ijkl}]\dot{E}_{kl}. \tag{2.23}$$

Note that $(N^{-1})_{\alpha\beta}$ refers to the $\alpha\beta$ element of the inverse of the submatrix of the matrix (N) corresponding to active compaction planes. An explicit expression for L is obtained by rearranging equations (2.18) and (2.23) into the form of equation (2.17) to get

$$L_{ijkl} = \mathscr{L}_{ijkl} - \sum_{\alpha=1}^{N}\sum_{\beta=1}^{N} [\mathscr{L}_{ijpq} T_{pq}^{(\alpha)} C^{(\alpha)} (N^{-1})_{\alpha\beta} T_{rs}^{(\beta)}\mathscr{L}_{rskl}]. \tag{2.24}$$

In the foregoing we have assumed that $\sigma_e^{(\alpha)}$ is a function of $\epsilon_e^{(\beta)}$. An alternative work hardening hypothesis is to assume normal hardening with no shear hardening, such that $\sigma_e^{(\alpha)}$ depends only upon $\epsilon^{(\beta)}$. For the case of independent hardening, the hardening matrix is then given by

$$h_{\alpha\alpha} = \frac{\sigma^{(\alpha)}}{\sigma_e^{(\alpha)}}\frac{d\sigma_e^{(\alpha)}}{d\epsilon^{(\alpha)}}$$

$$h_{\alpha\beta} = 0, \quad \alpha \neq \beta. \tag{2.25}$$

The above structure remains unchanged with this minor modification to the hardening rule. This form of hardening has been used by Schofield and Wroth [4] in their Cam Clay model and by Calladine [1] in his microstructural view of clay.

3. CALIBRATION OF CRYSTAL PLASTICITY LAW FOR ELLIPTICAL YIELD SURFACE

Ashby and co-workers (Helle *et al.* [5]) have developed accurate relations for the hydrostatic Stage I compaction of a powder aggregate. They assume that spherical particles are composed of elastic, perfectly-plastic material of yield strength σ_y. The yield pressure p_y for the aggregate is dependent

upon its relative density D (D = density of aggregate/full density) according to

$$p_y = 3D^2 \frac{(D - D_0)}{(1 - D_0)} \sigma_y \tag{3.1}$$

where D_0 is the initial relative density corresponding to random packing of the particles. For example, for dense random packing $D_0 = 0.64$.

We calibrate the hardening matrix $h_{\alpha\beta}$ in the crystal plasticity model against equation (3.1) in the hydrostatic limit. For simplicity, we assume independent hardening over N compaction planes so that $h_{\alpha\beta} = 0$ for $\alpha \neq \beta$; this is consistent with the notion that the contacts between particles act independently. We emphasise that the compaction planes are viewed as being smeared-out over the entire volume of the particle. For the case hydrostatic straining $\dot{E}^p_{kk}$ all planes α suffer identical normal straining with $\dot{\epsilon}^{(\alpha)} = \dot{E}^p_{kk}/N$, and $\sigma_e^{(\alpha)} = \sigma^{(\alpha)} = p_y$. The hardening rate $h_{\alpha\alpha}(\epsilon_e^{(\alpha)})$ for each compaction plane is given by

$$\dot{\sigma}_e^{(\alpha)} = h_{\alpha\alpha}(\epsilon_e^{(\alpha)}) \dot{\epsilon}_e^{(\alpha)} \quad \text{(no sum on } \alpha\text{)} \tag{3.2}$$

and is determined by comparing the time derivative of equation (3.1) with (3.2) to get

$$h_{\alpha\alpha}(\epsilon_e^{(\alpha)}) = \frac{3ND^2(3D - 2D_0)\sigma_y}{(1 - D_0)}. \tag{3.3}$$

For hydrostatic straining the relative density D is related to the effective strain $\epsilon_e^{(\alpha)}$ on each compaction plane by $D = D_0 e^{N\epsilon_e^{(\alpha)}}$, and so the diagonal terms $h_{\alpha\alpha}(\epsilon_e^{(\alpha)})$ of the hardening matrix may be rewritten as

$$h_{\alpha\alpha}(\epsilon_e^{(\alpha)}) = 3ND_0^3 e^{N\epsilon_e^{(\alpha)}} \frac{(3e^{N\epsilon_e^{(\alpha)}} - 2)}{1 - D_0} \sigma_y. \tag{3.4}$$

It remains to stipulate the shape of the yield surface for each compaction plane. A pragmatic approach is to assume the quadratic form of equation (2.7). Values for the constants $a^{(\alpha)}$ and $b^{(\alpha)}$ may be estimated from Green's [6] plane strain slip line field solution for the yield of a finite contact between two half-spaces. When the two half-spaces suffer a relative displacement of simple shear, the shear traction on the contact equals the shear yield strength k. In the other limit of pure normal approach (or separation) the magnitude of the normal traction equals the Prandtl field value of $(2 + \pi)k$. Thus, a first order estimate for $a^{(\alpha)}$ and $b^{(\alpha)}$ in equation (2.7) is $a^{(\alpha)} = b^{(\alpha)} = (2 + \pi)$. Although the shape of Green's [6] yield surface for a contact between two particles is not strictly elliptical in form, the quadratic approximation of equation (2.7) is a useful functional form as it avoids the difficulties associated with the vertex on the pressure axis of Green's yield surface.

A simpler limit yield surface for the compaction plane is to assume a closed polygon in stress space. A pragmatic approach is to assume that yield occurs when $\sigma^{(\alpha)}$ attains a limiting value $\sigma_t^{(\alpha)}$ in tension and $-\sigma_c^{(\alpha)}$ in compression, or when $|\tau^{(\alpha)}| = \tau_y^{(\alpha)}$, where $\tau_y^{(\alpha)}$ is the shear yield strength for the compaction plane

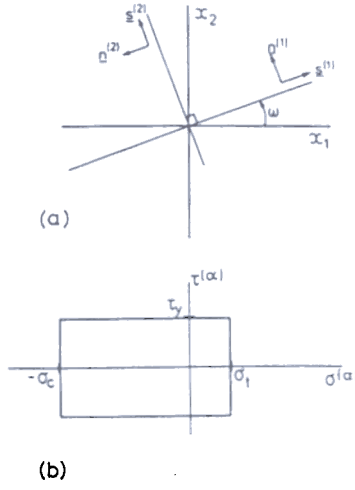

Fig. 2. (a) A pair of orthogonal compaction planes, with orientation ω. (b) Assumed yield surface for each compaction plane.

α, see Fig. 2(b). In the following section we use this simple algebraic form in order to gain insight into the relation between the local collapse response for each compaction plane and the macroscopic limit yield surface for the aggregate.

4. BISHOP–HILL CALCULATION OF YIELD SURFACE FOR HYDROSTATIC COMPACTION

So far we have dealt with the "single crystal response" of a finite set of compaction planes for a representative particle. Now consider the case of an aggregate comprising randomly oriented particles, bonded at their mutual contacts. The macroscopic "polycrystalline" limit yield surface for the aggregate of compaction planes can be estimated using the upper bound method laid down by Bishop and Hill [1]. Elastic deformation of the particles is ignored and a work calculation is performed to determine the collapse response in stress space for the random aggregate of particles. We restrict ourselves to in-plane biaxial straining of the aggregate, and assume that the deformation response for each particle is adequately described by a pair of orthogonal compaction planes, oriented at an angle ω as defined in Fig. 2(a). The aggregate is assumed to be isotropic, with the compaction planes distributed uniformly over all orientations.

For simplicity, we assume that the yield surface for each compaction plane is rectangular in shape as shown in Fig. 2(b), and is characterised by a compressive yield strength $\sigma_c^{(\alpha)}$, a tensile yield strength $\sigma_t^{(\alpha)}$ and a shear yield strength $\tau_y^{(\alpha)}$. The magnitude of the yield surface is taken to scale with the normal strain $\epsilon^{(\alpha)}$, such that

$$\sigma_e^{(\alpha)}(\epsilon^{(\alpha)}) = \sigma_c^{(\alpha)}. \tag{4.1}$$

Consider the case where an aggregate has been compacted hydrostatically from an initial density D_0

to a current density D. Then, the magnitude of $\sigma_c^{(\alpha)}$ for all compaction planes follows from equation (3.1) as

$$\sigma_c^{(\alpha)} = p_y = 3D^2 \frac{(D - D_0)}{(1 - D_0)} \sigma_y. \tag{4.2}$$

Gurson [7] has shown that the macroscopic stress Σ on the aggregate, corresponding to a plastic strain rate $\dot{E}^P$ is given by

$$\Sigma_{ij} = \frac{\partial W(\dot{E}^P)}{\partial \dot{E}^P_{ij}} \tag{4.3}$$

where W is the plastic dissipation rate of the aggregate per unit volume. It remains to estimate $W(\dot{E}^P)$. For a pair of orthogonal compaction planes as shown in Fig. 2(a), the plastic dissipation per unit volume w is

$$w = \sigma^{(1)}\dot{\epsilon}^{(1)} + \sigma^{(2)}\dot{\epsilon}^{(2)} + \tau^{(1)}\dot{\gamma}^{(1)} + \tau^{(2)}\dot{\gamma}^{(2)} \tag{4.4}$$

where we have dropped the subscript s from the shear terms, to keep notation compact. A simple connection exists between the strain rates on the compaction planes and the macroscopic strain rate; after some manipulation, equation (2.2) leads to

$$\begin{pmatrix} \dot{\epsilon}^{(1)} \\ \dot{\epsilon}^{(2)} \\ \dot{\gamma}^{(1)} - \dot{\gamma}^{(2)} \end{pmatrix} = \begin{pmatrix} \sin^2\omega & \cos^2\omega & -\sin 2\omega \\ \cos^2\omega & \sin^2\omega & \sin 2\omega \\ -\sin 2\omega & \sin 2\omega & 2\cos 2\omega \end{pmatrix} \begin{pmatrix} \dot{E}^P_{11} \\ \dot{E}^P_{22} \\ \dot{E}^P_{12} \end{pmatrix} \tag{4.5}$$

Since we are dealing with an isotropic aggregate we can consider principal stresses and principal strains and, without loss of generality, we can set $\dot{E}^P_{12} = 0$. For a given $(\dot{E}^P_{11}, \dot{E}^P_{22})$ the stress state for each of the two compaction planes is at a vertex, and both $\dot{\epsilon}^{(1)}$ and $\dot{\epsilon}^{(2)}$ are determined uniquely from equation (4.5) and from the minimum plastic work hypothesis of Bishop and Hill [2]: the strain rates are selected to minimise w. This optimisation gives $\dot{\gamma}^{(1)} > 0$, $\dot{\gamma}^{(2)} = 0$ for $(\dot{\gamma}^{(1)} - \dot{\gamma}^{(2)}) > 0$, and $\dot{\gamma}^{(1)} = 0$, $\dot{\gamma}^{(2)} > 0$ for $(\dot{\gamma}^{(1)} - \dot{\gamma}^{(2)}) < 0$.

The macroscopic stress Σ is calculated by volume averaging the response for a pair of compaction planes at all orientations, that is

$$\Sigma_{ij} = \frac{2}{\pi} \int_0^{\pi/2} \frac{\partial w}{\partial \dot{E}^P_{ij}} \, d\omega. \tag{4.6}$$

Upon substituting equations (4.4) and (4.5) into equation (4.6), we obtain an analytic specification for the yield surface

(i) $$\frac{\Sigma_{11}}{p_y} = \frac{\sigma_t}{\sigma_c} + \frac{2}{\pi}\frac{\tau_y}{\sigma_c}, \quad \frac{\Sigma_{22}}{p_y} = \frac{\sigma_t}{\sigma_c} - \frac{2}{\pi}\frac{\tau_y}{\sigma_c}$$

$$\text{for } \dot{E}^P_{11} > \dot{E}^P_{22} > 0 \tag{4.7a}$$

(ii) $$\frac{\Sigma_{11}}{p_y} = \frac{\sigma_t}{\sigma_c} - \frac{2}{\pi}\frac{\tau_y}{\sigma_c}, \quad \frac{\Sigma_{22}}{p_y} = \frac{\sigma_t}{\sigma_c} + \frac{2}{\pi}\frac{\tau_y}{\sigma_c}$$

$$\text{for } \dot{E}^P_{22} > \dot{E}^P_{11} > 0 \tag{4.7b}$$

(iii) $$\frac{\Sigma_{11}}{p_y} = -1 + \frac{2}{\pi}\frac{\tau_y}{\sigma_c}, \quad \frac{\Sigma_{22}}{p_y} = -1 - \frac{2}{\pi}\frac{\tau_y}{\sigma_c}$$

$$\text{for } \dot{E}^P_{22} < \dot{E}^P_{11} < 0 \tag{4.7c}$$

(iv) $$\frac{\Sigma_{11}}{p_y} = -1 - \frac{2}{\pi}\frac{\tau_y}{\sigma_c}, \quad \frac{\Sigma_{22}}{p_y} = -1 + \frac{2}{\pi}\frac{\tau_y}{\sigma_c}$$

$$\text{for } \dot{E}^P_{11} < \dot{E}^P_{22} < 0 \tag{4.7d}$$

(v) $$\frac{\Sigma_{11}}{p_y} = \frac{\sigma_t}{\sigma_c} - \frac{1}{\pi}\left(1 + \frac{\sigma_t}{\sigma_c}\right)(2\omega_1 - \sin 2\omega_1) + \frac{2}{\pi}\frac{\tau_y}{\sigma_c}$$

$$\frac{\Sigma_{22}}{p_y} = \frac{\sigma_t}{\sigma_c} - \frac{1}{\pi}\left(1 + \frac{\sigma_t}{\sigma_c}\right)(2\omega_1 + \sin 2\omega_1) - \frac{2}{\pi}\frac{\tau_y}{\sigma_c}$$

$$\text{for } \omega_1 = \arctan\sqrt{-\dot{E}^P_{22}/\dot{E}^P_{11}}$$

$$\text{and } \dot{E}^P_{11} > 0 > \dot{E}^P_{22} \tag{4.7e}$$

(vi) $$\frac{\Sigma_{11}}{p_y} = \frac{\sigma_t}{\sigma_c} - \frac{1}{\pi}\left(1 + \frac{\sigma_t}{\sigma_c}\right)(2\omega_1 + \sin 2\omega_1) - \frac{2}{\pi}\frac{\tau_y}{\sigma_c}$$

$$\frac{\Sigma_{22}}{p_y} = \frac{\sigma_t}{\sigma_c} - \frac{1}{\pi}\left(1 + \frac{\sigma_t}{\sigma_c}\right)(2\omega_1 - \sin 2\omega_1) + \frac{2}{\pi}\frac{\tau_y}{\sigma_c}$$

$$\text{for } \omega_1 = \arctan\sqrt{-\dot{E}^P_{22}/\dot{E}^P_{11}}$$

$$\text{and } \dot{E}^P_{22} > 0 > \dot{E}^P_{11}. \tag{4.7f}$$

The yield surface is plotted in Fig. 3 for the cases $\sigma_t/\sigma_c = 0$, 1 and $\tau_y/\sigma_c = 0$, $1/(2+\pi)$. The value $\tau_y/\sigma_c = 1/(2+\pi)$ corresponds to perfectly sticking contacts as discussed in Section 3. We conclude from Fig. 3 that the cohesive strength ratio σ_t/σ_c has a more major effect on the size and shape of the yield surface than has the shear strength ratio τ_y/σ_c. For a wide range of strain rate directions ($\dot{E}^P_{11} > 0$ and $\dot{E}^P_{22} > 0$; $\dot{E}^P_{11} < 0$ and $\dot{E}^P_{22} < 0$) the macroscopic stress lies at a vertex close to the hydrostatic axis. Akisanya

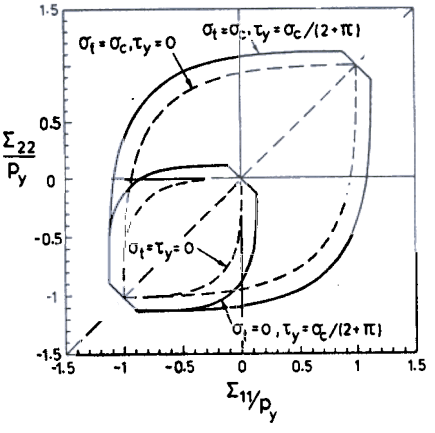

Fig. 3. Yield surface for a uniform distribution of an orthogonal pair of compaction planes, subjected to hydrostatic compaction.

and Cocks [8] observed a similar behaviour in their analysis of the compaction of a hexagonal array of cylindrical particles.

5. BISHOP–HILL CALCULATION OF YIELD SURFACE FOR CLOSED DIE COMPACTION: THE DEVELOPMENT OF ANISOTROPY

The above Bishop–Hill calculation can be repeated for the case of closed die compaction where, without loss of generality we take $E^p_{11} = 0$, $E^p_{22} < 0$. Again, we consider the response for an isotropic aggregate, composed of a uniform distribution of pairs of orthogonal compaction planes as shown in Fig. 2(a). The yield surface is taken to be rectangular in shape, see Fig. 2(b), and the magnitude of the yield surface scales with the normal strain $\epsilon^{(\alpha)}$ on that compaction plane, with $\sigma_c^{(\alpha)} = \sigma_c^{(\alpha)}(\epsilon^{(\alpha)})$.

Consider a compaction plane with orientation $\omega = 0$ such that the unit normal $n^{(1)}$ is aligned with the x_2 axis. The complementary compaction plane is orthogonal with a normal $n^{(2)}$ aligned with the x_1 axis. Then, after a small amount of closed die compaction (say $D = 0.7$ from an initial value of $D_0 = 0.64$), we have $\sigma_c^{(1)} = 2p_y$ and $\sigma_c^{(2)} = 0$, where $p_y(D)$ is given by equation (3.1).

For a pair of compaction planes with orientation ω, the normal strain on the compaction planes follows from equation (4.5) as

$$\epsilon^{(1)} = E^p_{22}\cos^2\omega, \qquad \epsilon^{(2)} = E^p_{22}\sin^2\omega. \tag{5.1}$$

We assume that the degree of compaction is small (D increases by less than 10%) and so the yield strengths ($\sigma_c^{(\alpha)}, \sigma_t^{(\alpha)}, \tau_y^{(\alpha)}$) and $\sigma_e^{(\alpha)}$ increase linearly with $\epsilon^{(\alpha)}$ for all compaction planes, giving

$$\sigma_c^{(1)} = 2p_y\cos^2\omega, \quad \sigma_c^{(2)} = 2p_y\sin^2\omega. \tag{5.2}$$

The shape of the yield surface for each compaction plane is taken to be constant with $\sigma_t^{(\alpha)}/\sigma_c^{(\alpha)}$ fixed at zero (for cohesionless aggregate) and at unity (for full cohesive strength). Perfectly sticking contacts are modelled by putting $\tau_y^{(\alpha)}/\sigma_c^{(\alpha)} = 1/(2+\pi)$, while the choice $\tau_y^{(\alpha)}/\sigma_c^{(\alpha)} = 0$ is appropriate for frictionless contacts.

The macroscopic yield surface is evaluated from equation (4.6), with w given by equation (4.4), and the strain rate for each compaction plane specified by (4.5). Again, the relative magnitudes of $\dot\gamma^{(1)}$ and $\dot\gamma^{(2)}$ are selected to minimise w, subject to the constraint on $(\dot\gamma^{(1)} - \dot\gamma^{(2)})$ given by equation (4.5). The macroscopic yield surface may be stated in closed form as

(i) $$\frac{\Sigma_{11}}{p_y} = \frac{1}{2}\frac{\sigma_t}{\sigma_c} + \frac{1}{\pi}\frac{\tau_y}{\sigma_c}, \quad \frac{\Sigma_{22}}{p_y} = \frac{3}{2}\frac{\sigma_t}{\sigma_c} - \frac{1}{\pi}\frac{\tau_y}{\sigma_c}$$
$$\text{for } \dot E^p_{11} > \dot E^p_{22} > 0 \tag{5.3a}$$

(ii) $$\frac{\Sigma_{11}}{p_y} = \frac{1}{2}\frac{\sigma_t}{\sigma_c} - \frac{1}{\pi}\frac{\tau_y}{\sigma_c}, \quad \frac{\Sigma_{22}}{p_y} = \frac{3}{2}\frac{\sigma_t}{\sigma_c} + \frac{1}{\pi}\frac{\tau_y}{\sigma_c}$$
$$\text{for } \dot E^p_{22} > \dot E^p_{11} > 0 \tag{5.3b}$$

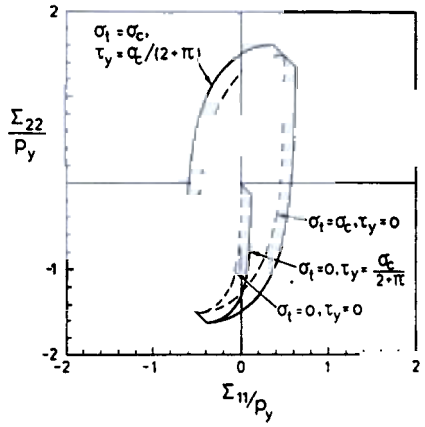

Fig. 4. Yield surface for a uniform distribution of an orthogonal pair of compaction planes, subjected to closed die compaction, $E^p_{11} = 0$, $E^p_{22} < 0$.

(iii) $$\frac{\Sigma_{11}}{p_y} = -\frac{1}{2} + \frac{1}{\pi}\frac{\tau_y}{\sigma_c}, \quad \frac{\Sigma_{22}}{p_y} = -\frac{3}{2} - \frac{1}{\pi}\frac{\tau_y}{\sigma_c}$$
$$\text{for } \dot E^p_{22} < \dot E^p_{11} < 0 \tag{5.3c}$$

(iv) $$\frac{\Sigma_{11}}{p_y} = -\frac{1}{2} - \frac{1}{\pi}\frac{\tau_y}{\sigma_c}, \quad \frac{\Sigma_{22}}{p_y} = -\frac{3}{2} + \frac{1}{\pi}\frac{\tau_y}{\sigma_c}$$
$$\text{for } \dot E^p_{11} < \dot E^p_{22} < 0 \tag{5.3d}$$

(v) $$\frac{\Sigma_{11}}{p_y} = \frac{1}{2}\frac{\sigma_t}{\sigma_c} - \frac{1}{\pi} + \frac{\sigma_t}{\sigma_c}\left(\omega_1 - \frac{1}{4}\sin 2\omega_1\right) + \frac{2}{\pi}\frac{\tau_y}{\sigma_c}$$
$$\frac{\Sigma_{22}}{p_y} = \frac{3}{2}\frac{\sigma_t}{\sigma_c} - \frac{1}{\pi}\left(1 + \frac{\sigma_t}{\sigma_c}\right) \times \left(3\omega_1 + 2\sin 2\omega_1 + \frac{1}{4}\sin 4\omega_1\right) - \frac{2}{\pi}\frac{\tau_y}{\sigma_c}$$
$$\text{for } \omega_1 = \arctan\sqrt{-\dot E^p_{22}/\dot E^p_{11}} \text{ and } \dot E^p_{11} > 0 > \dot E^p_{22} \tag{5.3e}$$

(vi) $$\frac{\Sigma_{11}}{p_y} = -\frac{1}{2} + \frac{1}{\pi}\left(1 + \frac{\sigma_t}{\sigma_c}\right)\left(\omega_1 - \frac{1}{4}\sin 2\omega_1\right) - \frac{2}{\pi}\frac{\tau_y}{\sigma_c}$$
$$\frac{\Sigma_{22}}{p_y} = -\frac{3}{2} + \frac{1}{\pi}\left(1 + \frac{\sigma_t}{\sigma_c}\right) \times \left(3\omega_1 + 2\sin 2\omega_1 + \frac{1}{4}\sin 4\omega_1\right) + \frac{2}{\pi}\frac{\tau_y}{\sigma_c}$$
$$\text{for } \omega_1 = \arctan\sqrt{-\dot E^p_{22}/\dot E^p_{11}} \text{ and } \dot E^p_{22} > 0 > \dot E^p_{11}. \tag{5.3f}$$

The yield surface for closed die compaction is plotted in Fig. 4 for $\sigma_t/\sigma_c = 0$, 1 and $\tau_y/\sigma_c = 0$, $1/(2+\pi)$. The main features are the same as for isostatic compaction, as shown in Fig. 3: the degree of cohesive strength has a major influence and the shear strength at the contacts has a minor influence upon the yield surface. As a result of preferential hardening of compaction planes aligned with the direction of compaction, significant anisotropy develops for closed die compaction. The compact is about three

times stronger in the compaction direction x_2 than in the transverse x_1 direction.

The yield surface for closed die compaction is compared with that for isostatic compaction in Fig. 5, for frictionless contacts ($\tau_y/\sigma_c = 0$) and for the two limiting cases of full cohesive strength ($\sigma_t/\sigma_c = 0$) and vanishing cohesive strength ($\sigma_t/\sigma_c = 0$). The comparison is made at the same value of relative density D slightly greater than D_0. The development of anisotropy under closed die compaction is obvious: the yield strength along the x_2 direction is greater after closed die compaction than after isostatic compaction. Conversely, the yield strength in the transverse direction is less for closed die compaction than for isostatic compaction.

6. CONCLUDING DISCUSSION

Fleck *et al.* [9] have previously used the Bishop–Hill method to estimate the macroscopic yield locus for Stage I compaction of a powder aggregate. They assume that plastic flow occurs in accordance with Green's [6] slip line field solution at all contacts on the surface of a representative spherical particle: all contacts are active for an arbitrary macroscopic strain rate. The contacts are assumed to be perfectly sticking with a cohesive strength equal to the indentation strength. More recently, Fleck [10] has repeated the calculation for a range of shear strength and cohesive strength. He finds that the macroscopic yield surface is influenced to a minor extent by the level of shear strength, and is much more strongly influenced by the cohesive strength. These conclusions are fully supported by the findings of the current study.

The predictions of Fleck [10] are compared with those of the current study in Fig. 6 for the case of isostatic compaction. Yield surfaces are given for frictionless contacts, with either zero cohesion or perfect cohesion between particles. The results are presented in terms of the deviatoric stress measure $\Sigma \equiv \Sigma_{22} - \Sigma_{11}$ and the mean stress measure $\Sigma_m \equiv \frac{1}{2}(\Sigma_{11} + \Sigma_{22})$, for the case of an isotropic distribution of two orthogonal compaction planes as described in Section 4. The calculation by Fleck [10] was done for axisymmetric loading of an aggregate with $\Sigma_{33} = \Sigma_{11}$; the appropriate deviatoric stress measure remains $\Sigma \equiv \Sigma_{22} - \Sigma_{11}$, and the mean stress is defined by $\Sigma_m \equiv \frac{1}{3}(\Sigma_{11} + 2\Sigma_{22})$. We conclude from Fig. 6 that the yield surface given by the plane strain crystal plasticity calculation of Section 4 and Fleck's [10] axisymmetric calculation (assuming plastic dissipation at up to twelve contacts per particle) give closely similar results. This is not surprising since both calculations assume that all contacts are active, and predictions have been calibrated to give the result of equation (3.1) for hydrostatic loading.

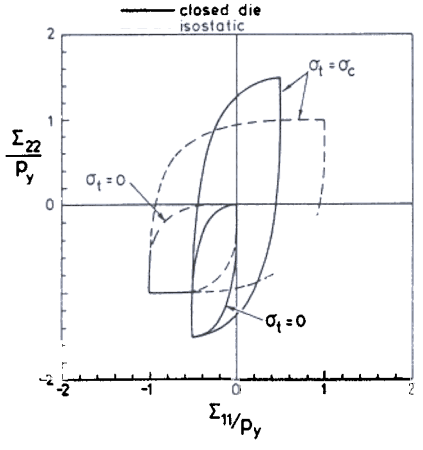

Fig. 5. Comparison of yield surface for isostatic compaction and for closed die compaction. The yield surfaces are calculated for the same small increment in relative density D above the initial density D_0. Contacts are frictionless with $\tau_y = 0$.

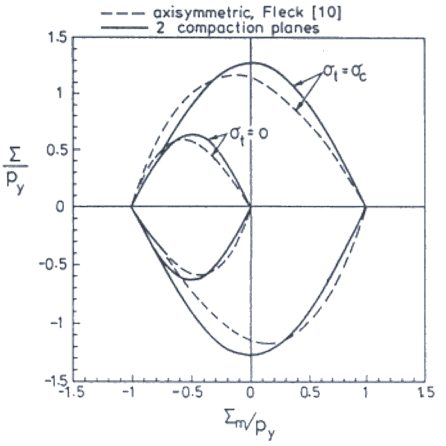

Fig. 6. Predictions of the yield surface after a small amount of hydrostatic compaction, for the two compaction plane model of the current study, and the axisymmetric model of Fleck [10]. Frictionless contacts.

The predictions of the crystal plasticity model are compared with the anisotropic model of Fleck [10] for the case of closed die compaction, see Fig. 7. Briefly, Fleck [10] assumed that the distribution of the number of contacts and area of each contact is distributed around the periphery of a representative particle in terms of a second order tensor B. Formulae are given for updating B with the macroscopic strain rate. Results for both models are given in Fig. 7 for frictionless contacts with either vanishing cohesive strength or full cohesive strength. Again, there is excellent agreement between the crystal plasticity calculation and the alternative anisotropic model. Available experimental data suggest that the anisotropic model of Fleck [10] gives predictions which are about 25% stronger than the observed response (see Ref. [10] for details). The crystal plasticity model gives a somewhat softer response than the Fleck [10] anisotropic model, in better agreement with the experimental data.

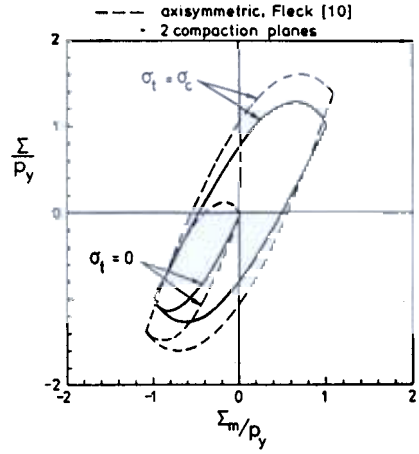

Fig. 7. Predictions of the yield surface after a small amount of closed die compaction, for the two compaction plane model of the current study, and the anisotropic model of Fleck [10]. $D = 0.7$, $D_0 = 0.64$, frictionless contacts.

Akisanya and Cocks [8] have recently examined the densification of a hexagonal array of cylinders under in-plane loading, and Ogbonna and Fleck [11] have performed an approximate calculation of axisymmetric compaction using a cell model. In both cases it is found that as densification proceeds plastic flow occurs throughout each particle and is no longer confined to each contact. Independent collapse of each contact is replaced by a discrete set of collapse mechanisms for the representative particle: these collapse mechanisms involve plastic dissipation at several contacts. Latent hardening occurs between one collapse mechanism and the next. The crystal plasticity framework has adequate flexibility to include this cross-hardening between mechanisms via the off-diagonal terms of the hardening matrix $h_{\alpha\beta}$. Further work is needed to further develop this calculation scheme.

The crystal plasticity framework appears to be an appropriate method for modelling the development of anisotropy during powder consolidation. The calculations suggest that strong anisotropy develops, with a vertex at the loading point. The crystal plasticity approach has the advantages that the macroscopic yield surface can be related to the local collapse mechanisms at the contacts, and the macroscopic tangent modulus can be written down for a given set of active compaction planes (i.e. for those contacts which are actively deforming).

Acknowledgements—The author is grateful for helpful discussions with A. C. F. Cocks, M. F. Ashby and A. Needleman. This work was supported by a contract (N00014-91-4089) with the Advanced Projects Agency and the Office of Naval Research, through a collaborative program with the University of Virginia.

REFERENCES

1. C. R. Calladine, *Geotechnique* **21**, 391 (1971).
2. J. W. F. Bishop and R. Hill, *Phil. Mag.* **42**, 414 (1951).
3. R. Hill, *J. Mech. Phys. Solids* **14**, 95 (1966).
4. A. N. Schofield and C. P. Wroth, *Critical State Soil Mechanics*. McGraw–Hill, London (1968).
5. A. S. Helle, K. E. Easterling and M. F. Ashby, *Acta metall.* **33**, 2163 (1985).
6. A. P. Green, *J. Mech. Phys. Solids* **2**, 197 (1954).
7. A. L. Gurson, *J. Engng Mater. Tech.* **99**, 2 (1977).
8. A. R. Akisanya and A. C. F. Cocks, *J. Mech. Phys. Solids*. **43**, 605 (1995).
9. N. A. Fleck, L. T. Kuhn and R. M. McMeeking *J. Mech. Phys. Solids* **40**, 1139 (1992).
10. N. A. Fleck, *J. Mech. Phys. Solids*. In press.
11. N. Ogbonna and N. A. Fleck, *Acta metall. mater.* **43**, 603 (1994).